

Application of Multi-path Ultrasonic Oil Flowmeter Using a New Weighting

Factor Method

Shang-Yoon Hwang and Ho-June Lee

Chang Min Tech Co., Ltd.

A-102, Bundang Techno Park, 150 Yatap, Bundang, Seongnam, 463-070, Korea

Heuy-Dong, Kim

School of Mechanical Engineering, Andong National University

388, Songchun, Andong, 760-749, Korea

Abstract Multi-path Ultrasonic Flowmeter(MUF) is receiving much attention because it provides a lot of advantages over other techniques of flow rate measurement. It has no moving parts inside flow passage leading to no pressure loss, and it gives a good accuracy and repeatability for flow rate measurement. The present study describes theoretical, experimental, and computational works to investigate the velocity integration method of MUF, which has five acoustic paths. A weighting factor concept, which is given by a function of the chord locations of acoustic paths, is employed to obtain the flowrate. In theoretical analysis, the power law velocity profiles are assumed for fully developed kerosene and water flow of the flow rate between $40 \text{ m}^3/\text{h}$ and $300 \text{ m}^3/\text{h}$. Computational analysis using 3-dimensional Navier-Stokes equations is performed to predict the velocity profiles in the flow passage and the results are validated with experimental data. The obtained result shows that for flowrate measurement of 5 paths ultrasonic oil flow meter, the present weighting factor concept gives good accuracy less than $\pm 0.14\%$.

Keywords: Multi-path ultrasonic flowmeter, Ultrasonic wave, Mean velocity, Weighting factor, Mass flow rate

1. Introduction

Determination of the mass flow rate of viscous fluid passing through a channel or a pipe is of practical importance in the aeronautical, automotive, chemical, and mechanical engineering industries since it is always associated with process control, transport of fluid, and energy consumption[1]. Ultrasonic wave has such characteristics as directivity, permeability, reflection, and refraction. It transmits well in liquid, gas as well as solid. Using these characteristics, a transit time of ultrasonic wave is of practical importance in obtaining local fluid velocity, consequently giving the flow rate of fluid.

Recently, ultrasonic flowmeter is receiving much

attention because it provides a lot of advantages over other techniques of flow rate measurement[2]. It has no moving parts inside flow passage, thus little pressure loss, good reliability and repeatability for a quite wide range of flow rates.

Ultrasonic flowmeter has been employed in a lot of industrial fields, such as water supply lines, wastewater lines, open channels, river flows, petroleum and natural gas flows, petrochemical, semiconductor process lines, etc. Its performance has been greatly improved with the recent development of digital signal processing[3]. In general, the flow rate measurement accuracy of MUF is influenced by fluid dynamic parameters, such as flow velocity profile[4], turbulent intensity[5], wall surface roughness [6], flow distortion[7], temperature gradient[8],

integration method of acoustic paths[9], ultrasonic transducer installation method[10], etc. Of these influencing factors, the most important uncertainty in the flow rate measurement stems from the velocity integration method, which is influenced by arrangement of acoustic paths and weighting factors to obtain local flow velocity relative to acoustic velocity of the ultrasonic signals. Since MUF is basically related to some numerical integration methods based upon a weighting factor or an interpolation, etc. It does not give detailed information related to the flow field.

The present study describes theoretical, computational, and experimental works to investigate the velocity integration method of MUF, which has five acoustic paths. A weighting factor method is employed to convert each of acoustic chord velocities along the ultrasonic paths to mean velocity and flow rate, and the weighting factors are given by functions of the chord locations of ultrasonic paths. In theoretical analysis, the power law velocity profiles are assumed for fully developed kerosene and water flow. Computational analysis is performed using the 3-dimensional Navier-Stokes equations. A fully implicit finite volume method is employed to numerically solve the governing equations. Experimentation is carried out to validate the present theoretical and computational results. In the present study, Reynolds number is varied to give kerosene flows with the flow rate between 60 m³/h and 300 m³/h, and water flows between 40 m³/h and 300 m³/h.

2. Measurement principal of MUF

Most of ultrasonic flowmeters use the transit time method of a pulse signal. As schematically illustrated in Figure 1, an ultrasonic beam propagates obliquely across the flow in the measurement pipe. Two ultrasonic transducers A and B, which may act as either transmitter or receiver, emit and detect short acoustic pulses alternatively. The time t_1 of the pulse transmitted downstream and t_2 of the pulse transmitted upstream are measured[11]. These are given as,

$$t_1 = \int_0^L \frac{dl}{C + V(l)\cos\theta} , \quad t_2 = \int_0^L \frac{dl}{C - V(l)\cos\theta} \quad (1)$$

,where C is the speed of sound and V is the local fluid velocity along ultrasonic paths in pipe. The velocity of the pulse signal propagation is $C + V \cos \theta = L/t_1$ downstream, and $C - V \cos \theta = L/t_2$ upstream, respectively, where L is the distance between the transducers and θ is the inclination angle to the flow direction. Using $\cos \theta = d/L$ and eliminating the speed of sound, which depends on the properties of the fluid, Eq.(1) is expressed as

$$V = \frac{L^2}{2d} \left(\frac{1}{t_1} - \frac{1}{t_2} \right) = \frac{L^2}{2d} \left(\frac{t_2 - t_1}{t_1 \cdot t_2} \right) \quad (2)$$

Thus, the fluid velocity V depends only on well known geometrical factors and the times t_1 and t_2 which are to be measured. Since, $\Delta t = t_2 - t_1$ is very short compared with t_1 or t_2 , a precise integration method is necessary to obtain the fluid velocity with good accuracy.

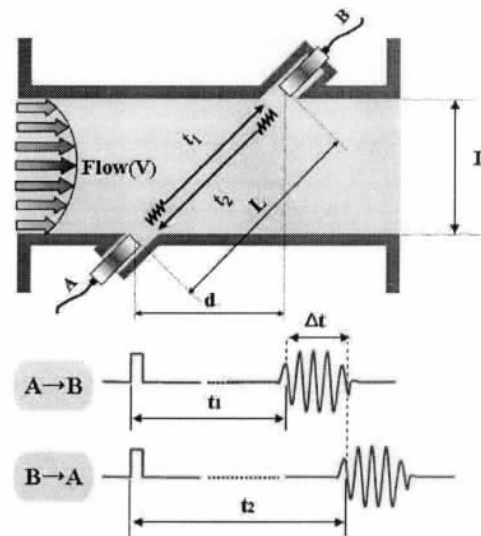


Fig.1 Schematic illustration of metering principle of MUF

3. Analytical method

The power law velocity profile for a fully developed pipe flow is yielded to simulate the velocity profile integration method. Figure 2 shows typical turbulent velocity profiles, in which Reynolds number

is varied between 10^4 and 10^8 for a hydro-dynamically smooth pipe. These velocity profiles are given as the power law equation as,

$$\frac{V}{V_{\max}} = \left(1 - \frac{r}{R}\right)^{1/n} \quad (3),$$

where V_{\max} is the velocity on the centerline of pipe, R is the radius of pipe, and n is the power index, which depends strongly on Reynolds number.

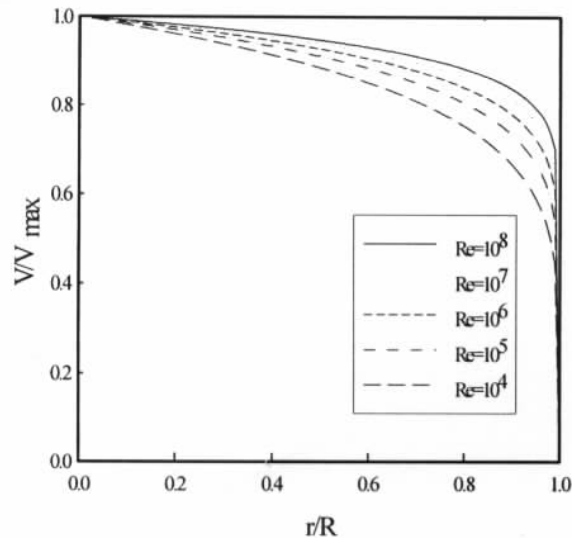


Fig.2 Typical turbulent velocity profiles for pipe flow

Eq.(3) fits most of fully developed turbulent velocity profiles, but it can be unsatisfactory near the wall and on centerline. The power index n can be given by friction coefficient f , which is also a function of Reynolds number, and relative roughness k , as follows[6],

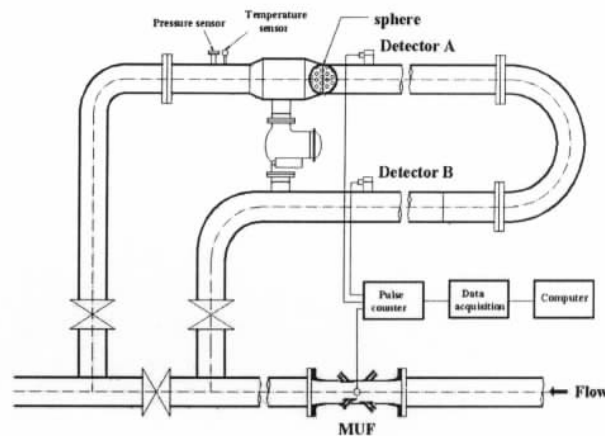
$$n = \frac{1}{\sqrt{f}} = 1.74 - 2 \log_{10} \left(2 \frac{k}{D} + \frac{18.7}{Re \sqrt{f}} \right) \quad (4)$$

3.2. Computational method

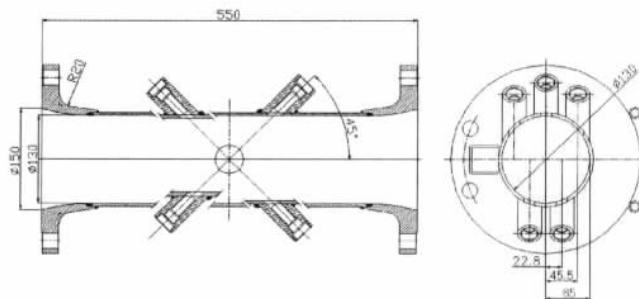
The flow field of MUF, a computational analysis is performed using 3-dimensional, steady, incompressible, Navier-Stokes equations, which are solved by a fully finite volume scheme, is based upon the second order upwind scheme for spatial derivatives and Multi-stage Runge-Kutta method for time derivatives. The standard

k-ε model is used to predict viscous stresses. The working fluid is kerosene and water. Regarding the boundary conditions, pipe inlet and outlet are applied to uniform velocity and outflow condition. The computational domain is extended up to 7D upstream from the pipe inlet and 25D downstream from the pipe outlet. A structured grid system of 150,000 nodes is applied to the present pipe. The calculated results are used for the purpose of comparison with theoretical results of the line average velocities along the ultrasonic paths.

4. Experimental method



(a) Experimental test rig



(b) Ultrasonic flow meter for 5-paths

Fig.3 Schematic diagram of experimental rig and MUF

Figure 3 shows schematic diagram of the experimental test rig and detailed MUF, which has 5-ultrasonic paths. Ultrasonic transducers, which have a resonance frequency of 850 kHz, are installed onto the test pipe wall at an inclination angle of 45 degree to the pipe centerline. Their positions are located at 22.8 mm,

45.5 mm from a centerline. The test pipe has a contraction part upstream of the MUF and a divergent part downstream. A novel calibration device for measuring flow rate uses a pipe prover system. It is installed upstream of the by-pass flow passage. The pipe prover system consists of a sphere drifting along the fluid flow inside the pipe. The sensors to detect the sphere movement are installed into the pipe wall, and the movement distance is measured to obtain the flow rate.

Meanwhile, a pulse counter connected with the detecting sensors and MUF controller measures the number of pulses to obtain the flow rate during the test, and a data acquisition system converts the measured pulses to volumetric flow rate of fluid. In experiment, kerosene and water are employed and their flow rates are varied between 40 m³/h and 300 m³/h.

4. Velocity integration method

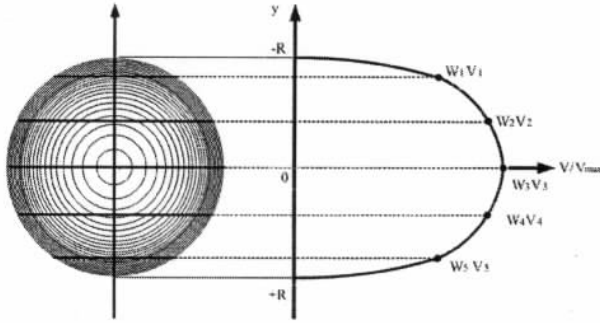


Fig.4 Schematic of velocity integration method

Figure 4 presents the velocity integration method along the ultrasonic paths. From the measured transit times of the ultrasonic signals, a batch of 35 point velocities is averaged along the ultrasonic chords to obtain the line averaged velocity, as follows,

$$V_i = \frac{1}{L} \int_{\text{chord}} v(l) dl \quad (5)$$

The summation of the resulting line averaged velocities and weighing factors is defined as a mean velocity, as follows,

$$V_{\text{mean}} = \sum_{i=1}^5 W_i V_i \quad (6),$$

where

$$W_1 = \frac{A(d_3 d_4 + d_3 d_5 + d_4 d_5 - d_2 d_3 - d_2 d_4 - d_2 d_5) - B d d_3 d_4 d_5 + C}{(1-d_1^2)^k (d_1 - d_2)(d_1 + d_3)(d_1 + d_4)(d_1 + d_5)}$$

$$W_2 = \frac{A(d_3 d_4 + d_3 d_5 + d_4 d_5 - d_1 d_3 - d_1 d_4 - d_1 d_5) - B d d_3 d_4 d_5 + C}{(1-d_2^2)^k (d_2 - d_1)(d_2 + d_3)(d_2 + d_4)(d_2 + d_5)}$$

$$W_3 = \frac{A(d_1 d_2 + d_4 d_5 - d_1 d_4 - d_1 d_5 - d_2 d_4 - d_2 d_5) + B d d_2 d_4 d_5 + C}{(1-d_3^2)^k (d_1 + d_3)(d_2 + d_3)(d_3 - d_4)(d_3 - d_5)}$$

$$W_4 = \frac{A(d_1 d_2 + d_3 d_5 - d_1 d_3 - d_1 d_5 - d_2 d_3 - d_2 d_5) + B d d_2 d_3 d_5 + C}{(1-d_4^2)^k (d_1 + d_4)(d_2 + d_4)(d_4 - d_3)(d_4 - d_5)}$$

$$W_5 = \frac{A(d_1 d_2 + d_3 d_4 - d_1 d_3 - d_1 d_4 - d_2 d_3 - d_2 d_4) + B d d_2 d_3 d_4 + C}{(1-d_5^2)^k (d_1 + d_5)(d_2 + d_5)(d_5 - d_3)(d_5 - d_4)}$$

,where subscripts 1, 2, 3, 4 and 5 are the numbers indicating the positions of ultrasonic transducers, and A, B, C, and k is the constants to be employed in the weighting factor, d is the distance from the pipe wall to each of ultrasonic transducers. Using V_{mean} value in Eq.(6), the flow rate of the fluid is obtained as,

$$Q = \frac{\pi D^2}{4} \cdot V_{\text{mean}} \quad (7)$$

Table.1 is the list of the constants employed in Eq.(6).

Table 1 The constants used in weighting factor

A	0.335918				
B	1.468630				
C	0.158153				
k	0.186000				
d_i / R	path 1	path 2	path 3	path 4	path 5
	0.70	0.35	0.00	0.35	0.70
W_i	0.2344	0.0466	0.4302	0.0466	0.2344

5. Results and discussion

Figure 5 shows axial velocity profile and a comparison between line average velocities obtained from CFD and from power law velocity profile.

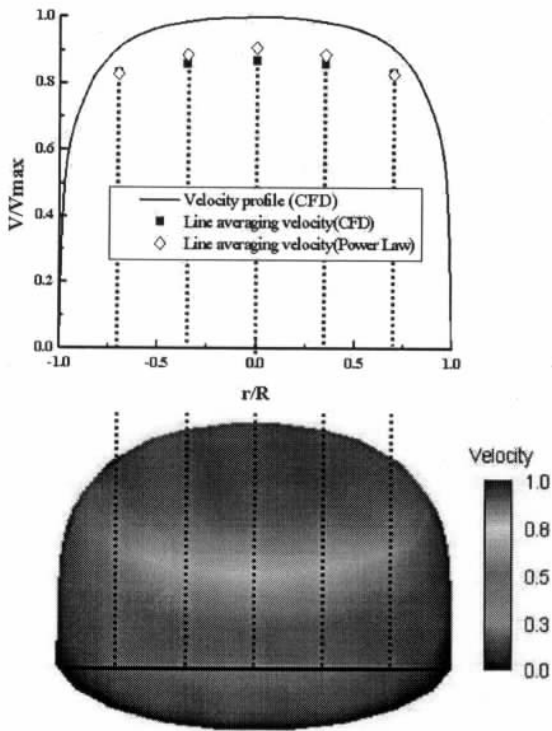


Fig.5 Axial velocity profile and line averaged velocity for theoretical and CFD results (Re=365,915, Kerosene)

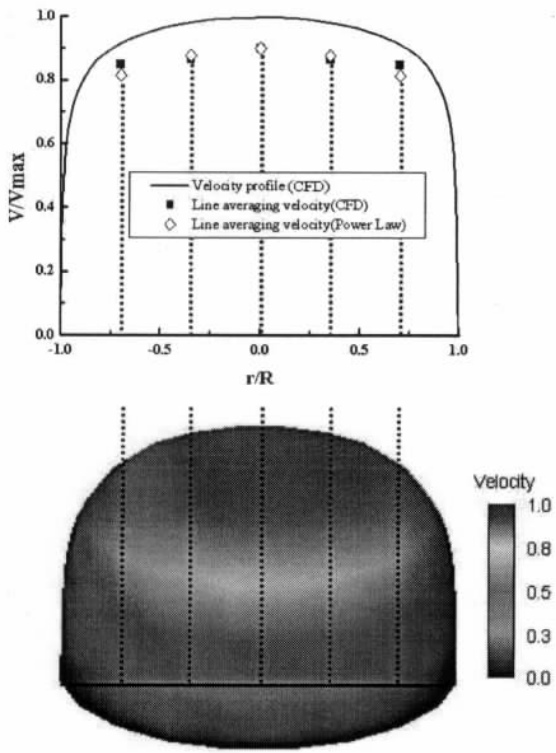


Fig.6 Axial velocity profile and line averaged velocity for theoretical and CFD results (Re=657,883, Water)

The working fluid is kerosene at $Re=365,915$. V/V_{max} means the local velocity divided by the maximum velocity on the pipe centerline. Line average velocity calculated from the power law velocity profiles predicts the present CFD results well, although it somewhat overpredicts the CFD results on the centerline.

For water flow at $Re=657,883$, Figure 6 shows the axial velocity profiles. The power law velocity profile is in quite close agreement with the CFD result. However, the agreement very near the pipe wall is slightly poor. Thus, it is believed that the present power law can be appropriately used for the purpose of obtaining the velocity profiles for fully developed pipe flows.

Figure 7 represents the effect of the pipe wall roughness on the velocity integration method using power law velocity profile. For a given k/D , the present integration error decreases as Reynolds number increases, while for a given Reynolds number the integration error decreases with an increase in k/D . The difference between the maximum and minimum values of the velocity integration errors appears much smaller as k/D increases. From the present results, the velocity integration error is estimated to be about $\pm 0.3\%$ for the ranges of $Re=10^4$ to 10^8 and of $k/D=0$ to 10^{-2} .

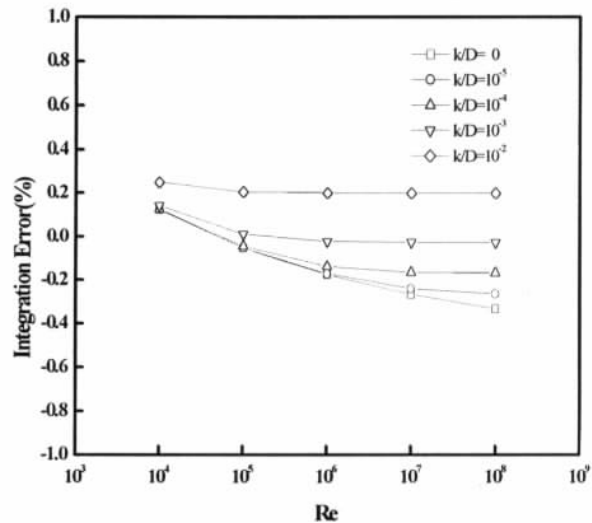


Fig.7 Effect of wall surface roughness on velocity integration method

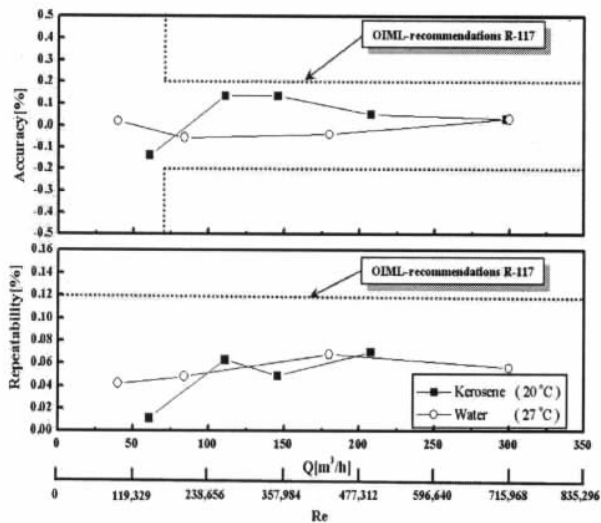


Fig.8 Accuracy and repeatability

Figure 8 shows the present experimental results of the accuracy and repeatability. The measurement accuracy and repeatability for kerosene and water flows are estimated by $\pm 0.14\%$, $\pm 0.07\%$, and $\pm 0.08\%$, $\pm 0.07\%$, respectively. This result is quite acceptable for the OIML Recommendations R-117.

6. Conclusion

The present study describes the velocity integration method of 5-paths ultrasonic oil flowmeter. The present velocity integration method uses a weighting factor concept to obtain the flow rate of incompressible viscous flows through a pipe. In the present study, theoretical and computational works are performed, and validated with the measured results. The weighting factors are given by functions of the chord locations of acoustic paths. The present velocity integration method, using the power law profile, predicts well the computational and measured profiles for fully developed kerosene and water flows which are in the flow rate range from $40 \text{ m}^3/\text{h}$ and $300 \text{ m}^3/\text{h}$. The obtained result shows that for flow rate measurement of 5-paths ultrasonic oil flowmeter, the present weighting factor concept provides a good accuracy less than $\pm 0.14\%$ in kerosene and $\pm 0.08\%$ in water, respectively.

Reference

- [1] H. Koechner, A. Melling. Numerical Simulation of Ultrasonic Flowmeters. *ACUSTICA*, Vol. 86, 2000, pp. 39~48.
- [2] M. Takamoto, H. Ishikawa, K. Shimizu, H. Monji, G. Matsui. New measurement method for very low liquid flow rates using ultrasound. *Flow Measurement and Instrumentation* 12, 2001, pp. 267~273.
- [3] H. Ishikawa, M. Takamoto, K. Shimizu, G. Matsui. The effect of beam width on ultrasonic flowmeter performance, *Proceedings of FLOMEKO'98*, Sweden, 1998, pp.137~142.
- [4] M.V. Zagarola, A.J. Smits. Scaling of the mean velocity profile for turbulent pipe flow. *Physical Review Letters* 78(2), 1997, pp.239~242.
- [5] B. Iooss, C. Lhuillier, H. Jeanneau. Numerical simulation of transit-time ultrasonic flowmeter: uncertainties due to flow profile and fluid turbulence. *Ultrasonic* 40, 2002, pp. 1009~1015.
- [6] A. Calogirou, J. Boekhoven, R.A.W.M. Henkes. Effect of wall roughness changes on ultrasonic gas flowmeters. *Flow Measurement and Instrumentation* 12, 2001, pp. 219~229.
- [7] Pamela I Moore, Gregor J Brown, Brian P Stimpson. Ultrasonic transit-time flowmeters modeled with theoretical velocity profiles: methodology. *Meas. Sci. Technol* 11, 2000, pp.1802~1811.
- [8] M. Willatzen. Ultrasonic flowmeters: temperature gradients and transducer geometry effects. *Ultrasonic* 41, 2003, pp.105~114.
- [9] J. Halttunen, E. Lunttaa. Comparison of different weighting methods of multipath ultrasonic flowmeter. *Proceedings of the Australasian Instrumentation and Measurement Conference*, Auckland, New Zealand, 1992, pp. 369~372.
- [10] C. Carlander, J. Delsing. Installation effects on an ultrasonic flowmeter. *Proceedings FLOMEKO'98*, 1998.
- [11] M. Willatzen. Ultrasound transducer modeling – general theory and applications to ultrasound reciprocal systems, *IEEE Trans. Ultrasonics, Ferroelectrics Freq. Control* 48, 2001, pp. 100~112.